

**Fluorescent and Photoconductive Nanoribbons as Dual-mode Sensor for  
Selective Discrimination of Alkyl Amines versus Aromatic Amines**

Yibin Zhang, Cheng Peng, Xiaojie Ma, Yanke Che\*, Jincal Zhao

Key Laboratory of Photochemistry, Institute of Chemistry, Chinese Academy of Sciences,  
Beijing 100080, China.

Email: [ykche@iccas.ac.cn](mailto:ykche@iccas.ac.cn)

### **Synthesis and assembly of molecules 1.**

The synthesis of molecules **1** and the fabrication of the nanoribbons were performed following our previously reported procedure.<sup>1, 2</sup> The pure compound of **1** was obtained through running column chromatography on a silica gel column, for which chloroform was used as eluent. The pure target compound as obtained were confirmed by <sup>1</sup>HNMR and MALDI-MS as below.

<sup>1</sup>HNMR (300 MHz, CDCl<sub>3</sub>) δ 8.64-8.73 (m, 8H, perylene), 7.55 (d, J = 9.6 Hz, 2H, phenyl), 6.85 (d, J = 9.6 Hz, 2H, phenyl), 5.36 (s, 2H, CH<sub>2</sub>), 4.21 (t, J = 7.6 Hz, 2H, CH<sub>2</sub>), 3.77 (s, 3H, OCH<sub>3</sub>), 1.71-1.77 (m, 2H, CH<sub>2</sub>), 1.25-1.38 (m, 18H, 9CH<sub>2</sub>), 0.85-0.87 (m, 3H, CH<sub>3</sub>).

MALDI-MS: (m/z) 678.2.

### **Fabrication of the nanoribbons from 1.**

The nanoribbons from **1** was assembled by injecting 0.5 mL of a chloroform solution of the compound (0.15 mM) into 5 mL of ethanol in a test tube followed by 3 days of aging. The nanoribbons thus formed can be transferred and cast onto a glass slide by pipetting. We fabricated the nanoribbon film by dropping-casting 300 μL 10 μg/mL solution of nanoribbons suspending in ethanol onto a glass slide (deposition area is about 1 cm<sup>2</sup>). We used AFM to estimate the thickness of the nanoribbon film on the glass slide and found the film thickness is not uniform, ranging from 150 to 500 nm.

### **Morphology and Property Characterizations.**

UV-vis absorption spectra of the monomer in chloroform and nanoribbons from **1** suspended in ethanol were measured on a PerkinElmer Lambda 35 spectrophotometer. The fluorescence spectrum of the nanoribbons from **1** deposited on a glass slide were measured on an Ocean Optics USB4000 fluorometer using a 455 nm LED lamp as the light source. The fluorescence quantum yield of the nanoribbons was determined by the integrating sphere method performed on Hamamatsu Absolute PL Quantum Yield spectrometer C11247. AFM measurements of the nanoribbons were performed in the tapping mode on a Bruke MultiMode V scanning probe microscope. TEM measurements were performed with FEI Tecnai G2 T20 (120KV). Electron spin resonance (ESR) measurements were performed with a Bruker ESP-300E spectrometer under the settings of center field, 3480.00 G, microwave frequency, 100.0 KHz, power, 10.3 mW. The deaerated samples were prepared upon encapsulation of the capillary coated by the nanoribbons into a NMR tube which is followed by being sealed in the argon-filled glove box. Photocurrent measurements of the nanoribbons were carried out through a simple two-probe method (electrode: 20 μm long and 3 μm wide) using a probe station and Agilent B1500A semiconductor parameter analyzer for high-resolution current measurement. A tungsten lamp (150 W) was used as the light source to excite the nanoribbons.

### **Fluorescent and photoconductive sensing measurements.**

The time-dependent fluorescence quenching profile was obtained with an Ocean

Optics USB4000 fluorometer. The fluorescence quenching was carried out by blowing 5 mL of amine vapors at certain concentration onto the nanoribbon film with a syringe at the speed of 2 mL/s during the course when the emission was continuously recorded by the fluorometer. A 455 nm LED light source was used to excite the nanoribbons. Photoconductive changes of the nanoribbons from **1** when exposed to the blowing amine vapors (with a syringe at the speed of 2 mL/s ) were recorded at the bias of 10 V under whit light irradiation (30 mW/cm<sup>2</sup>). A tungsten lamp (150 W) was used as the light source to excite the nanoribbons.

**Supplementary figures.**

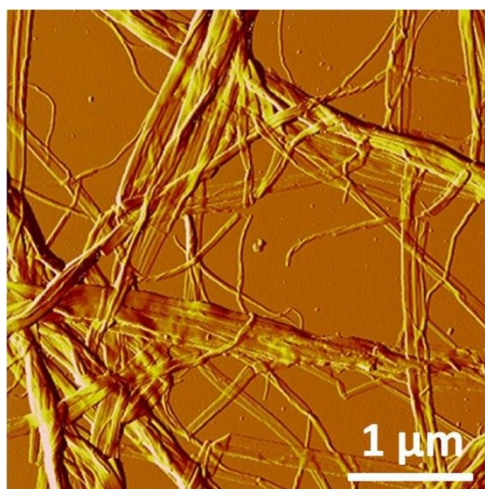


Figure S1. AFM images (Amplitude mode) of the bilayer nanoribbons from **1**, clearly showing bundles of nanoribbons.

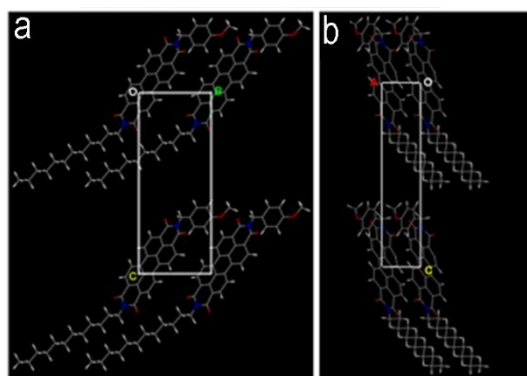


Figure S2. Molecular packing of **1** within the microribbon viewed from the (100) and (010), respectively.

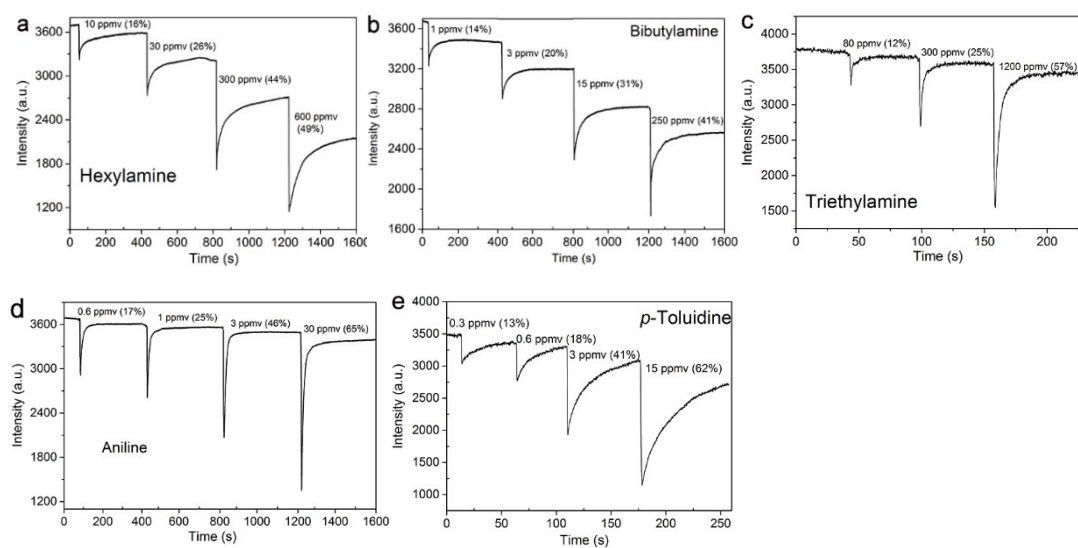


Figure S3. Concentration-dependent fluorescent responses of the nanoribbons from **1** upon exposure to hexylamine (a), bibutylamine (b), trimethylamine (c), aniline (d), and *p*-toluidine vapor.

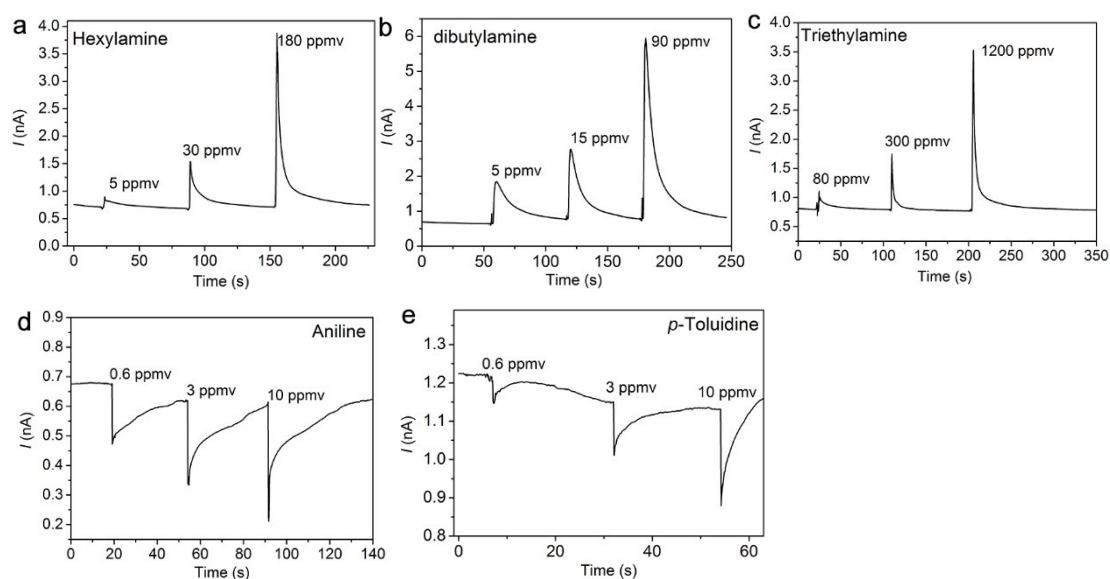


Figure S4. Concentration-dependent photoconductive responses of the nanoribbons from **1** upon exposure to hexylamine (a), bibutylamine (b), trimethylamine (c), aniline (d), and *p*-toluidine vapor.

1. Y. Che, X. Yang, G. Liu, C. Yu, H. Ji, J. Zuo, J. Zhao and L. Zang, *J. Am. Chem. Soc.*, 2010, **132**, 5743-5750.
2. X. Liu, Y. Zhang, X. Pang, E. Yue, Y. Zhang, D. Yang, J. Tang, J. Li, Y. Che and J. Zhao, *J. Phys. Chem. C*, 2015, **119**, 6446-6452.